# On a finite difference scheme for solving the non-linear primitive equations for a barotropic fluid with application to the boundary current problem

By GÜNTER FISCHER, *Meteorologisches Institut der Universität Hamburg, Germany*

(Manuscript received April 22, 1965)

ABSTRACT

In this paper a finite difference scheme for solving the primitive equations for a barotropic fluid is proposed. This scheme is an extension of a method investigated thoroughly by the author in a recent paper (1965). It has certain advantages against the commonly used leap frog scheme insofar as it occupies less space in the computer and avoids fictitious numerical solutions. To test the finite difference scheme computations are performed with an ocean model where the circulation is generated by a prescribed meridional distribution of zonal winds. The $\beta$-plane approximation has been applied. The solutions behaved well and showed no instabilities.

## 1. Introduction

In a recent paper, "A survey of finite difference approximations to the primitive equations" the author (Fischer, 1965) has investigated the accuracy and stability properties of several finite difference approximations to the primitive equations. The primitive equations were used in a simplified linearized form for a one-dimensional barotropic fluid on a non-rotating earth. Among the different schemes, the scheme denoted 1b had some interesting aspects, that makes it worth-while to study it in more detail. It has also been investigated by Kasahara (1965).

The advantages against the commonly used leap frog scheme lie in the fact that the future fields at time $t+\Delta t$ are only dependent on the past fields at time $t$, whereas the leap frog scheme requires the additional knowledge of the fields at time $t-\Delta t$; the order of accuracy is the same in both schemes. Moreover, Ib excludes the occurrence of fictitious solutions which may be generated in the leap frog scheme, since this approximates also a differential equation of higher order in time than the original one (Platzman, 1958). In the simplified form it could be shown that Ib is stable in the sense of von Neumann and possesses for long waves a slight damping proportional to $U^2/m^4$, where $U$ is the particle velocity and $m=L/\Delta s$ is the number of grid intervals $\Delta s$ representing the wave length $L$. The stability condition can be written: $2\ U^2\Delta t^2/\Delta s^2+\gamma^2\Delta t^2/\Delta s^2\leqslant 1$ where $\gamma$ is the phase velocity of gravity waves. For the shortest possible wave length $L=2\ \Delta s$ the amplification factor becomes equal to: $1-2\ U^2\Delta t^2/\Delta s^2$.

Thus there is an artificial damping of the shortest wave length, the damping decreases, however, sharply with increasing m. According to Richtmyer (1963) this artificial damping will probably help to avoid the non-linear instability observed by Phillips (1959) in the neutrally stable leap frog scheme, since it removes the wave energy from the short waves where it is accumulated by passing from longer to shorter wave lengths.

## 2. The mathematical model

In this paper the main object is to describe an extension of Ib to a system of equations that govern the motion of a non-linear barotropic fluid in a rotating frame. In order to prove that the scheme works satisfactorily examples are presented for the development of wind-induced currents in a $\beta$-plane ocean of simple rectangular shape, simulating a similar model treated by Bryan (1963).

It is hoped that a consistent extension of Ib to two dimensions in space including the coriolisforces and forcing functions will retain the stability properties, though it was not possible to give an exact analytic proof because of the complicated nature of the difference equations.

The system of differential equations which govern the motions of a barotropic viscous fluid reads as follows:

$$\frac{\partial u}{\partial t} = -\mathbf{v}\cdot\nabla u + fv - \frac{\partial \phi}{\partial x} + A\nabla^2 u + \frac{\tau_1}{\bar{h}}, \quad (1\,a)$$

$$\frac{\partial v}{\partial t} = -\mathbf{v}\cdot\nabla v - fu - \frac{\partial \phi}{\partial y} + A\nabla^2 v + \frac{\tau_2}{\bar{h}}, \quad (1\,b)$$

$$\frac{\partial \phi}{\partial t} = -\nabla\cdot(\mathbf{v}\phi) - g\bar{h}\nabla\cdot\mathbf{v}, \quad (1\,c)$$

$\mathbf{v}$ is the vector for the velocity of the fluid with the components $u$ and $v$ in the $x$- and $y$-direction respectively; $\phi$ denotes the geopotential of the fluid surface relatively to the mean height $\bar{h}$; $\tau_1$ and $\tau_2$ are the windstress components in the $x$- and $y$-direction respectively; $A$ is the coefficient of lateral diffusion, $f$ the coriolis parameter dependent linearly on the latitude. The bottom stress is assumed to vanish. $\nabla$ is the horizontal del-operator.

## 3. The finite difference equations

In approximating the differential system to a system of finite difference equations the following symbols are used:

$$u_{j,k}^{(n)} \equiv u(j\Delta x,\ k\Delta y,\ n\Delta t): \quad \Delta x = \Delta y = \Delta s,$$

where

$(x,y) = (j\Delta x,\ k\Delta y)$ is a gridpoint,

$$j = 0,\ \pm\tfrac{1}{2},\ \pm 1,\ \pm\tfrac{3}{2}\ \ldots;\ k = 0,\ \pm\tfrac{1}{2},\ \pm 1,\ \pm\tfrac{3}{2}\ \ldots,$$

$$n = 0, 1, 2\ \ldots,$$

$$\bar{u}^x \equiv \tfrac{1}{2}(u_{j+\frac{1}{2},k} + u_{j-\frac{1}{2},k}),$$

$$\bar{u}^y \equiv \tfrac{1}{2}(u_{j,k+\frac{1}{2}} + u_{j,k-\frac{1}{2}}),$$

$$\bar{u} \equiv \tfrac{1}{2}(\bar{u}^x + \bar{u}^y),$$

$$u_x \equiv (u_{j+\frac{1}{2},k} - u_{j-\frac{1}{2},k}),$$

$$u_y \equiv (u_{j,k+\frac{1}{2}} - u_{j,k-\frac{1}{2}}),$$

$$\nabla\cdot\mathbf{v} \equiv u_x + v_y,$$

$$\bar{\mathbf{v}}\cdot\nabla u \equiv \bar{u}u_x + \bar{v}u_y.$$

We want to apply both a time- and space-staggered scheme, where the velocity and the geopotential are prescribed at different time levels and at different grid points. We shall prescribe $u$ and $v$ at integer times and at grid points for which $j+k$ have integer values. On the other hand $\phi$ is specified at half odd integer times and grid points for which $j+k$ have half odd integer values. We shall compute the new fields $u^{(n+1)}$, $v^{(n+1)}$ from the old fields $u^{(n)}$, $v^{(n)}$ and $\phi^{(n+\frac{1}{2})}$. Thereafter the new field $\phi^{(n+\frac{3}{2})}$ is obtained from $\phi^{(n+\frac{1}{2})}$ and the just before derived $u^{(n+1)}$, $v^{(n+1)}$. This procedure is quite economic as it uses the latest information. Consequently less fields have to be stored in the computer than is the case for the leap frog scheme. It is essential that all terms on the right hand side of (1a), (1b) and (1c) appear, when transformed into finite difference form, at the central time with respect to each equation. Only in this case the required accuracy and computational stability can be ascertained. Since the variables given at the respective central times do not correspond directly with our basic values $u^{(n)}$, $v^{(n)}$ and $\phi^{(n+\frac{1}{2})}$ we have to introduce some additional techniques in order to achieve this effect indirectly.

We write first our finite difference equation in the following form:

$$u_{j,k}^{(n+1)} - \frac{f\Delta t}{2} v_{j,k}^{(n+1)}$$

$$= u_{j,k}^{(n)} - \frac{\Delta t}{\Delta s}(\bar{\mathbf{v}}^*\cdot\nabla u^*)^{(n+\frac{1}{2})} + \frac{f\Delta t}{2} v_{j,k}^{(n)} - \frac{\Delta t}{\Delta s}\phi_x^{(n+\frac{1}{2})}$$

$$+ \frac{A\Delta t}{\Delta s^2}\nabla^2 u^{(n)} + \frac{\Delta t}{\bar{h}}\tau_1^{(n+\frac{1}{2})} \equiv \tilde{u}_{j,k}^{(n+1)};$$

$$j+k = 0,\ \pm 1,\ \pm 2\ \ldots, \quad (2\,a)$$

$$v_{j,k}^{(n+1)} + \frac{f\Delta t}{2} u_{j,k}^{(n+1)}$$

$$= v_{j,k}^{(n)} - \frac{\Delta t}{\Delta s}(\bar{\mathbf{v}}^*\cdot\nabla v^*)^{(n+\frac{1}{2})} - \frac{f\Delta t}{2} u_{j,k}^{(n)} - \frac{\Delta t}{\Delta s}\phi_y^{(n+\frac{1}{2})}$$

$$+\frac{A\Delta t}{\Delta s^2}\nabla^2 v^{(n)} + \frac{\Delta t}{\bar{h}}\tau_2^{(n+\frac{1}{2})} \equiv \tilde{v}_{j,k}^{(n+1)};$$

$$j+k=0, \pm 1, \pm 2 \ldots, \quad (2\text{b})$$

$$\phi_{j,k}^{(n+\frac{3}{2})} = \phi_{j,k}^{(n+\frac{1}{2})} - \frac{\Delta t}{\Delta s}\nabla\cdot(\mathbf{v}\phi^*)^{(n+1)} - \frac{g\bar{h}\Delta t}{\Delta s}\nabla\cdot\mathbf{v}^{(n+1)};$$

$$j+k=\pm\tfrac{1}{2}, \pm\tfrac{3}{2} \ldots. \quad (2\text{c})$$

Note that the coriolisforces have been introduced in a semi-implicit way in order to appoint them at the central time. They have been written as $fv_{j,k}^{(n+\frac{1}{2})} = \frac{1}{2} f(v_{j,k}^{(n)} + v_{j,k}^{(n+1)})$; $-fu_{j,k}^{(n+\frac{1}{2})} = -\frac{1}{2} f(u_{j,k}^{(n)} + u_{j,k}^{(n+1)})$ and the "unknowns" $-\frac{1}{2} f\Delta t\, v_{j,k}^{(n+1)}$; $\frac{1}{2} f\Delta t\, u_{j,k}^{(n+1)}$ have been added to the left hand side of (2a) and (2b). Excluding the non-linear terms denoted by a $*$-superscript, which shall be treated later separately, it is now possible to deduce from the basic values $u^{(n)}$, $v^{(n)}$ and $\phi^{(n+\frac{1}{2})}$, assumed to be known, the right hand sides of (2a) and (2b) thus $\tilde{u}_{j,k}^{(n+1)}$ and $\tilde{v}_{j,k}^{(n+1)}$ are known. Since $u_{j,k}^{(n+1)}$, $v_{j,k}^{(n+1)}$ are given at the same grid points they can easily be derived from (2a) and (2b) by solving an inhomogeneous equation. This yields:

$$u_{j,k}^{(n+1)} = \frac{1}{1+\frac{1}{4}f^2\Delta t^2}\{\tilde{u}_{j,k}^{(n+1)} + \tfrac{1}{2}f\Delta t\, \tilde{v}_{j,k}^{(n+1)}\}, \quad (2\text{d})$$

$$v_{j,k}^{(n+1)} = \frac{1}{1+\frac{1}{4}f^2\Delta t^2}\{\tilde{v}_{j,k}^{(n+1)} - \tfrac{1}{2}f\Delta t\, \tilde{u}_{j,k}^{(n+1)}\}. \quad (2\text{e})$$

Thus $u_{j,k}^{(n+1)}$ and $v_{j,k}^{(n+1)}$ are computed (in the linear case!) and serve in the last equation (2c) to evaluate the new field for the geopotential $\phi^{(n+\frac{3}{2})}$. Thus in the linear system our requirement is fulfilled, namely that we only need the knowledge of the fields at one distinct time in order to compute the new fields. It can be shown that the linear system with $A=0$, $\tau_1=\tau_2=0$ and $f=$const. has neutral stability, provided:

$$g\bar{h}\frac{\Delta t^2}{\Delta s^2} \leq \tfrac{1}{2}.$$

In certain respects this finite difference scheme is very similar to one employed by the author (Fischer, 1959) in tidal computation. The main difference which is quite important, is the different formulation of the coriolisterm and the gridsystem.

So far the non-linear terms have not been considered. They have also to be introduced into our finite difference system at the respective central time. Unfortunately, however, our variables are not specified directly—as was the case for the coriolisterms—at this time and we have therefore called these fictitious values $u^{*(n+\frac{1}{2})}$, $v^{*(n+\frac{1}{2})}$, $\phi^{*(n+1)}$. It shall be stressed once more that it is important to evaluate all terms —except the frictional terms—on the right hand side of the system (1) in finite difference form at the central time, even though the time level is not the same in the $u$-, $v$- and $\phi$-equation respectively. The only exception is the frictional term which should be applied, as is well known, at the old time.

Consequently our next aim is to express the non-linear terms through our basic values. To achieve this we could employ an implicit method. It is more convenient, however, to follow a procedure by Lax & Wendroff (1960) and expand $u^{*(n+\frac{1}{2})}$, $v^{*(n+\frac{1}{2})}$ and $\phi^{*(n+1)}$ into a Taylor series around $t=n\,\Delta t$ and $t=(n+\frac{1}{2})\,\Delta t$ respectively. We retain only those terms which guarantee the desired accuracy and approximate the values in finite difference form with respect to the gridpoints for the basic variables. This gives for $u^{*(n+\frac{1}{2})}$, for example:

$$u_{j,k}^{*(n+\frac{1}{2})} = \bar{u}^{(n)} + \left\langle\frac{\partial u}{\partial t}\right\rangle_{j,k}^{(n)}\frac{\Delta t}{2}; \quad j+k=\pm\tfrac{1}{2}, \pm\tfrac{3}{2}, \ldots.$$

Here $\langle\partial u/\partial t\rangle_{j,k}^{(n)}$ denotes an appropriate finite difference approximation to $\partial u/\partial t$ in (1a). A corresponding procedure is used for $v^{*(n+\frac{1}{2})}$ and $\phi^{*(n+1)}$. This gives the following by-equations, which are only employed to evaluate the non-linear terms:

$$u_{j,k}^{*(n+\frac{1}{2})} = \bar{u}^{(n)} - \tfrac{1}{2}\frac{\Delta t}{\Delta s}(\bar{\mathbf{v}}\cdot\nabla u)^{(n)} + \frac{f\Delta t}{2}\bar{v}^{(n)}$$

$$-\tfrac{1}{2}\frac{\Delta t}{\Delta s}\bar{\phi}_x^{(n+\frac{1}{2})} + \tfrac{1}{2}\frac{A\Delta t}{\Delta s^2}\nabla^2\bar{u}^{(n)} + \tfrac{1}{2}\frac{\Delta t}{\bar{h}}\tau_1^{(n)}, \quad (2\text{f})$$

$$v_{j,k}^{*(n+\frac{1}{2})} = \bar{v} - \tfrac{1}{2}\frac{\Delta t}{\Delta s}(\bar{\mathbf{v}}\cdot\nabla v)^{(n)} - \frac{f\Delta t}{2}\bar{u}^{(n)} - \tfrac{1}{2}\frac{\Delta t}{\Delta s}\bar{\phi}_y^{(n+\frac{1}{2})}$$

$$+\tfrac{1}{2}\frac{A\Delta t}{\Delta s^2}\nabla^2\bar{v}^{(n)} + \tfrac{1}{2}\frac{\Delta t}{\bar{h}}\tau_2^{(n)}, \quad (2\text{g})$$

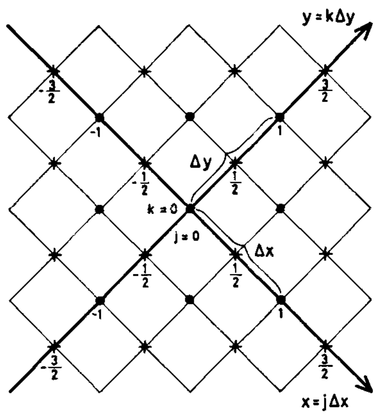


FIG. 1. Coordinate system and distribution of gridpoints in the $x$, $y$-plane. $u$, $v$, $\phi^*$ are prescribed at integer-times at ●-points; $\phi$, $u^*$, $v^*$ are prescribed at half odd integer times at $+$-points.

$$\phi^{*(n+1)}_{j,k} = \overline{\phi}^{(n+\frac{1}{2})} - \tfrac{1}{2}\frac{\Delta t}{\Delta s}\,\nabla\cdot(\overline{\mathbf{v}}^{(n+1)}\phi^{(n+\frac{1}{2})})$$

$$-\tfrac{1}{2}\frac{g\overline{h}\Delta t}{\Delta s}\,\nabla\cdot\overline{\mathbf{v}}^{(n+1)}. \quad (2\text{h})$$

$u^{*(n+\frac{1}{2})}_{j,k}, v^{*(n+\frac{1}{2})}_{j,k}$ shall be specified at gridpoints $j+k=\pm\frac{1}{2}, \pm\frac{3}{2}, \ldots$ and $\phi^{*(n+1)}_{j,k}$ at gridpoints $j+k=0, \pm 1, \pm 2, \ldots$.

Now our goal has been reached, namely to express $u^{(n+1)}$ by $u^{(n)}$, $v^{(n)}$, $\phi^{(n+\frac{1}{2})}$; $v^{(n+1)}$ by $u^{(n)}$, $v^{(n)}$, $\phi^{(n+\frac{1}{2})}$ and finally $\phi^{(n+\frac{3}{2})}$ by $u^{(n+1)}$, $v^{(n+1)}$ $\phi^{(n+\frac{1}{2})}$. That this is really so can best be seen when the variables $u^*$, $v^*$, $\phi^*$ in (2a), (2b), (2c) are eliminated through (2f), (2g), (2h). But this has not been done in favour of a clearer representation, because in practice it is certainly more convenient to apply the finite difference equations in several steps. To avoid unnecessary storage the equations (2f), (2g) and (2h) should really be used as by-equations in order to evaluate the non-linear terms when they are needed for a certain gridpoint; i.e. not the whole $u^*$, $v^*$, $\phi^*$-fields should be stored in the computer.

To repeat briefly the procedure that should be obeyed in order to arrive at the future fields: Stored in the computer are the basic fields $u^{(n)}$, $v^{(n)}$, $\phi^{(n+\frac{1}{2})}$; then (2a) and (2b) together with (2d) and (2e) allow with the aid of (2f) and (2g) to compute $u^{(n+1)}$ and $v^{(n+1)}$. These new values replace the old values for the velocity since the latter are not needed anymore. Now we have stored $u^{(n+1)}$, $v^{(n+1)}$, $\phi^{(n+\frac{1}{2})}$ and are thus able to derive from (2c) with the aid of (2h) $\phi^{(n+\frac{3}{2})}$. This new value for the geopotential replaces the old value and we arrive thus at the new basic fields: $u^{(n+1)}$, $v^{(n+1)}$, $\phi^{(n+\frac{3}{2})}$ and can repeat whole the procedure in order to get the values at any desired time.

The distribution of gridpoints shows Fig. 1. Accordingly $u$, $v$, $\phi^*$ are prescribed at gridpoints where $j+k$ have integer values and $\phi$, $u^*$, $v^*$ are prescribed at gridpoints where $j+k$ have half odd integer values. This distribution of gridpoints permits a good approximation of space derivatives. Unfortunately the $x$, $y$-coordinates do not point parallel or perpendicular to those grid points for which $j+k$ is either an integer value or a half odd integer value. For specifying the boundary values which are constraints on the velocity or the geopotential it would have been more convenient to place the $x$-axis and $y$-axis parallel and/or perpendicular to the boundaries, which in any case should only run through points where either $u$, $v$, $\phi^*$ or $\phi$, $u^*$, $v^*$ are prescribed. Otherwise there arise difficulties in evaluating the boundary conditions in the numerical scheme. This shortcoming could easily be eliminated by turning the coordinate system by 45° and by transforming the finite difference equations to this new sys-

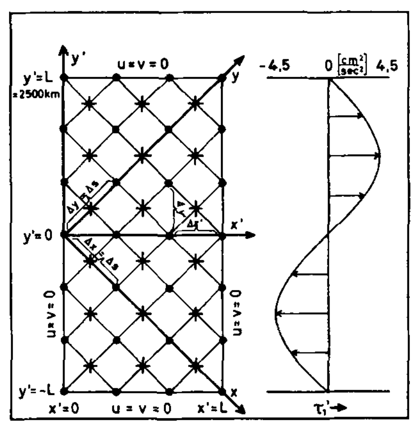


FIG. 2. The horizontal configuration of the model ocean with distribution of gridpoints. The computations are performed in the $x$, $y$-coordinate system (see also Fig. 1). At all boundaries non-slip conditions were applied. The right hand side shows the meridional distribution of the zonal windstress.

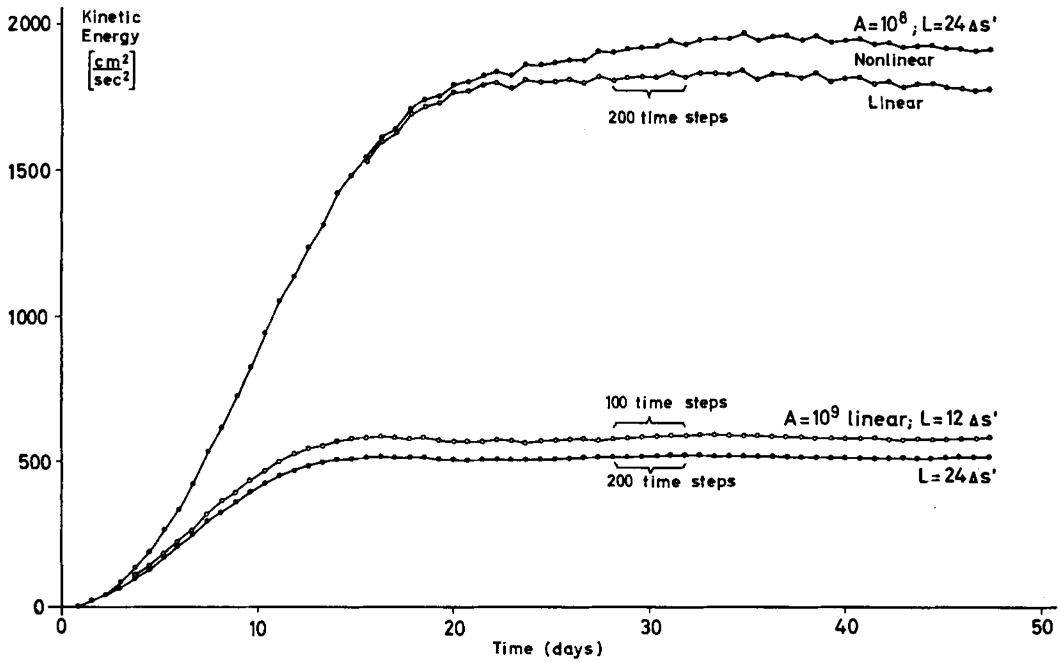


FIG. 3. Variation of mean kinetic energy with time for varying model assumptions under the influence of a constant windstress, when the system is initially at rest.

tem. This is, however, not necessary and has not been done in the present computations, i.e. the coordinate system has an angle of 45° against the rectangular boundaries.

## 4. Discussion of the numerical model

Regarding the computations for a wind-induced ocean circulation which were performed with the finite difference equations a rectangular ocean with the width $L$ in zonal direction and a meridional extension of $2L$ has been applied. At all boundaries non-slip conditions were prescribed, i.e. both the tangential and normal component of the velocity shall vanish at the boundaries; this implies that $u = v = 0$. In order to facilitate the explanation of the model we shall adopt a coordinate system where the $x'$-axis points eastward and the $y'$-axis northward. Correspondingly we shall designate $u'$, $v'$ and $\tau_1'$, $\tau_2'$ as the $x'$, $y'$-components of the velocity and windstress respectively. Note, however, that the computations were performed with the $x$, $y$-coordinate system; the shape of the ocean, the coordinate systems and the sinusoidial distribution of the windstress are shown in Fig. 2. The mean depth of the ocean is assumed to be 200 m and should be interpreted as the depth of the main thermocline rather than the actual depth of the ocean, because the main circulation is concentrated above the thermocline. The boundaries cross those points where $u$, $v$, $\phi^*$ are prescribed. Since $u = v = 0$ no computations of the flow were applied at the boundaries, neither is it necessary to compute $\phi^*$ at the boundaries as its value appears in the equation (2c) multiplied with the velocity, which vanishes there. The only difficulty arises in connection with the evaluation of the differences $\bar{\phi}_x$ and $\bar{\phi}_y$ in the equations (2f) and (2g) at grid-points next to the boundaries. This requires the knowledge of $\phi$-values outside the boundaries. To get these values a linear interpolation from values inside has been employed. The coriolis-parameter is a linear function of latitude, thus: $f = f_0 + \beta y'$. The numerical values are as follows:

$L = 2500$ km,
$\bar{h} = 200$ m,
$f_0 = 0.975\ 10^{-5}$ sec$^{-1}$,
$\beta = 1.5\ 10^{-13}$ sec$^{-1}$ cm$^{-1}$,

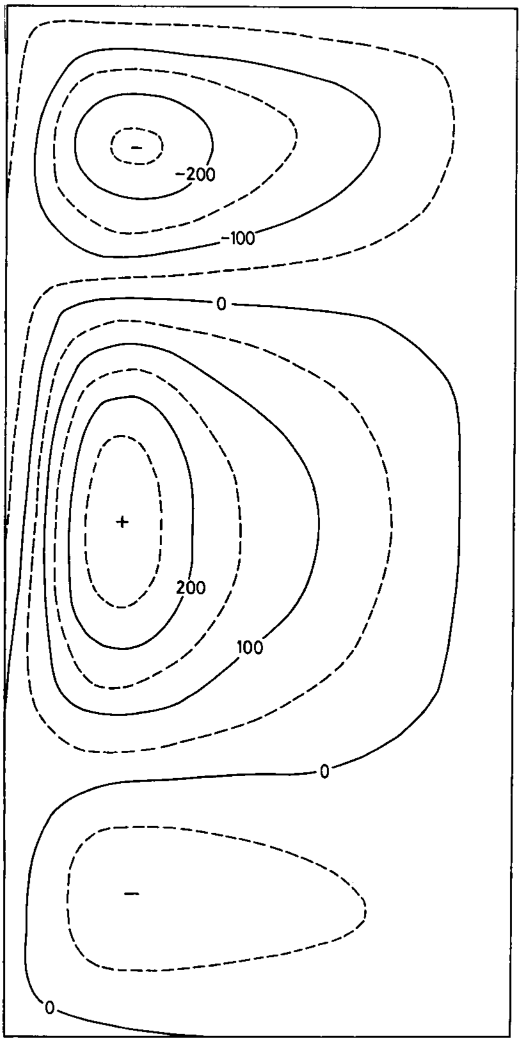


FIG. 4. Patterns of the surface height $\phi/g$ for $A = 10^9$ cm$^2$ sec$^{-1}$ derived from the linear equations after the equilibrium state is reached ($t = 2560\ \Delta t$). The non-linear solution is about the same.

$A = 10^9$ or $10^8$ cm$^2$ sec$^{-1}$,
$\tau_1' = -4.5 \sin \Pi y'/L$ cm$^2$ sec$^{-2}$ $-L \leqslant y' \leqslant +L$,
$\tau_2' = 0$,
$\Delta s' = L/12$ or $L/24$,
$\Delta t = \frac{1}{2}(g\,\bar{h})^{-\frac{1}{2}}\,\Delta s$.

This model is very similar to one employed by BRYAN (1963). There the main weight was placed on the physical aspects of the model with respect to the gulf stream. Our main concern is to illustrate more the technical bearings of the finite difference scheme and the computations shall only serve to show the feasibility to get stable solutions. The differences against Bryan's model are that he used a windstress proportional to sin $\Pi y'/2L$ in the range $-L \leqslant y' \leqslant +L$ and a slip condition at the northern and southern boundary, i.e. $v' = 0$, $\partial u'/\partial y' = 0$ at $y' = \pm L$. Another difference refers to the numerical scheme: Bryan employed the non-divergent barotropic vorticity equation in finite difference form to compute the stream function for the wind-induced flow.

The computations start from a state of rest; then the prescribed windstress sets up a circulation. After a certain number of time steps a steady state is expected to be reached when the energy input by the windstress compensates the energy loss by frictional dissipation. In the linear case this steady state should obey the equations:

$$\beta v' = \frac{\text{curl}\ \tau'}{\bar{h}} + A\nabla^2\left(\frac{\partial v'}{\partial x'} - \frac{\partial u'}{\partial y'}\right),$$

$$\frac{\partial u'}{\partial x'} + \frac{\partial v'}{\partial y'} = 0; \quad \left(\text{curl}\ \tau' = \frac{\partial \tau_2'}{\partial x'} - \frac{\partial \tau_1'}{\partial y'}\right).$$

This equation was studied by MUNK 1950 with the famous result that under the influence of zonal winds the $\beta$-term together with the lateral diffusion generates a boundary current along the western boundary whose width is dependent on the parameter $(A/\beta)^{\frac{1}{3}}$. Munk's solution for the meridional component $v'$ was assumed to be proportional to $-\partial\tau_1'/\partial y'$. Unfortunately this solution does not apply to our model since it does not satisfy the boundary condition at the northern and southern boundary. In our model $-\partial\tau_1'/\partial y'$ does not vanish at $y' = \pm L$ whereas the velocity component $v'$ is forced through the boundary conditions to do so. An exact comparison between the linear Munk solution and our linear numerical solution is therefore not possible. In fact, it turned out that along $y' = 0$ our numerical solution for the linear case showed differences against the Munk solution even though the deviations were relatively small. Because our numerical solution did alter only slightly when the net was refined it is believed that truncation errors play a minor role and cannot be attributed for the observed differences.

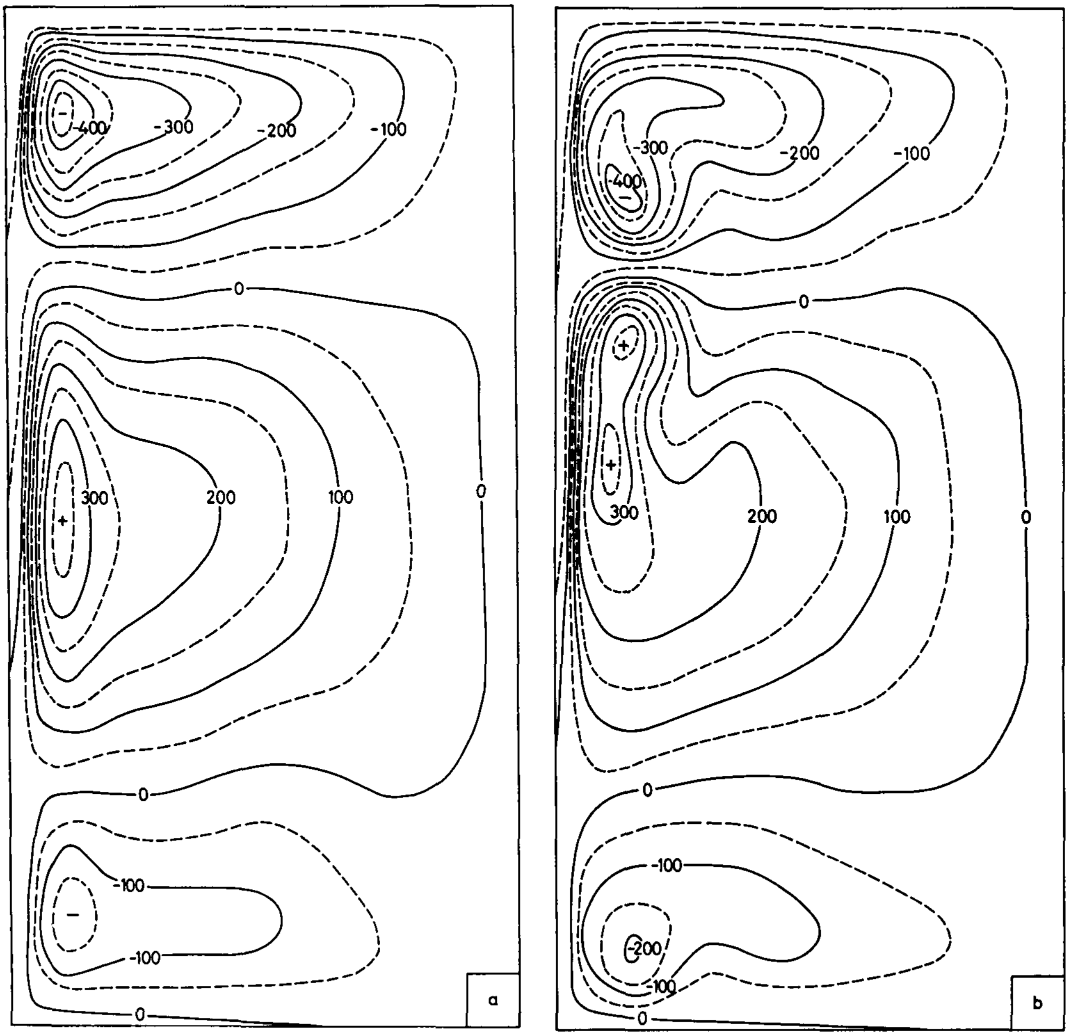


FIG. 5. Patterns of the surface height $\phi/g$ for $A = 10^8$ cm² sec⁻¹; (*a*) solution obtained from the linear equations; (*b*) solution obtained from the non-linear equations ($t = 2560\ \Delta t$).

## 5. Discussion of the solutions

Several cases with varying magnitude of the coefficient of viscosity A and varying mesh length were studied; both the linear and non-linear version were computed in order to show how the fields are changed through the incorporation of the non-linear terms. Only those cases which may deserve some interest are selected to be presented in this paper.

Fig. 3 displays the evolution in time of the mean kinetic energy for $A = 10^9$ cm$^2$ sec$^{-1}$ and $A = 10^8$ cm$^2$ sec$^{-1}$; it is clearly seen that in both cases a near equilibrium state is reached. That was not possible anymore for a coefficient of viscosity as low as $10^7$ cm$^2$ sec$^{-1}$ for a grid $\Delta s' = L/24$; there the mean kinetic energy increased all the time (up to 2560 time steps) and the flow was broken up into several small cells. Using Bryan's definition for the Reynolds number Re and the Rossby number $\varepsilon$, the values for our model become $\mathrm{Re} = 47\ 10^8/A$ ($A$ measured in cm$^2$ sec$^{-1}$) and $\varepsilon = 2\ 10^{-3}$. Bryan too was not able to reach a steady state for such high Reynolds number as $A = 10^7$ cm$^2$ sec$^{-1}$ would give. Maybe a further refinement of the net that could represent the rather narrow boundary current whose width should be in the order of 1 $\Delta s'$ would deliver a more plausible solution. More probably, however, there exists no real steady state anymore for such a low number of lateral diffusion. For $A = 10^8$ cm$^2$ sec$^{-1}$ the equilibrium level for the mean kinetic energy is a little higher for the non-linear case than for the linear both curves show smaller fluctuations. Also the grid distance has some influence on the solution as can be seen for the energy curves for $A = 10^9$ cm$^2$ sec$^{-1}$. Unfortunately there are no values which allow a comparison of different grid distances for the energy curves for $A = 10^8$ cm$^2$ sec$^{-1}$.

Fig. 4 shows the height field $\phi/g$ in cm (height relative to the mean sea surface) for $A = 10^9$ cm$^2$ sec$^{-1}$ (Re $= 4.7$; $\varepsilon = 2\ 10^{-3}$) and $\Delta s' = L/24$. In this case there exists nearly no difference between the linear and non-linear solution, therefore only the linear field has been presented. The flow is quasi-geostrophic, thus the lines of constant height can approximately be considered as streamlines. Apart from the regions near the northern and southern boundaries the solution corresponds qualitatively to Munk's solution; the boundary current near the western boundary is strongest where $-\partial\tau_1'/\partial y'$ has its maximum value, i.e. at $y' = 0$. The width of the boundary current was about 5 $\Delta s'$.

More interesting is the height field for $A = 10^8$ cm$^2$ sec$^{-1}$ (Re $= 47$; $\varepsilon = 2\ 10^{-3}$). Fig. 5*a* gives the linear solution, whereas Fig. 5*b* shows the non-linear solution. Here clearly distinguishable differences occur between the two height fields. The linear solution for $\phi/g$ is more or less symmetric around the line $y' = 0$. This symmetry is lost in the non-linear case which gives a strong countercurrent with a wave-like form north of the region of maximum wind curl at $y' = 0$. The center of maximum height is shifted northward and possesses an elongated form. This result corresponds very well with Bryan's numerical solution for the same magnitude of Re and $\varepsilon$, though the two models are not quite identical. In this case the width of the boundary current is represented by 3 $\Delta s'$.

It would have been desirable to repeat the computations with Bryan's model assumptions in order to get the possibility of an exact comparison; moreover the linear Munk solution could have been applied in this case. Unfortunately, for personal reasons, this was not possible and we must be satisfied with the results presented here. They show in any case that the finite difference method described in this paper can well be applied to solve the non-linear primitive equations.

## 6. Acknowledgements

The author wishes to thank the National Center for Atmospheric Research in Boulder/Colorado to give him permission to use the computer facilities. Thanks are especially extended to Mr. F. Nagle for writing the machine program and for performing the computations on his own initiative.

## REFERENCES

Bryan, K., 1963, A numerical investigation of a nonlinear model of a wind-driven ocean. *J. Atm. Sciences*, vol. **20**, No. 6, pp. 594–606.

Fischer, G., 1959, Ein numerisches Verfahren zur Errechnung von Windstau und Gezeiten in Randmeeren. *Tellus*, vol. **11** No. 1, pp. 60–76.

Fischer, G., 1965, A survey of finite-difference approximations to the primitive equations. *Monthly Weather Rev.*, vol. **93**, No. 1, pp. 1–10.

Kasahara, A., 1965, On certain finite difference methods for fluid dynamics. *Monthly Weather Rev.*, vol. **93**, No. 1, pp. 27–31.

Lax, P. D., and Wendroff, B., 1960, Systems of conservation laws. *Communications on Pure and Applied Mathematics*, vol. **13**, pp. 217–237.

Munk, W. H., 1950, On the wind-driven ocean circulation. *J. Meteor.*, vol. **7**, No. 2, pp. 79–93.

Platzman, G., 1958, The lattice structure of the finite-difference primitive and vorticity equations. *Monthly Weather Rev.*, vol. **86**, No. 8 pp. 285–292.

Phillips, N. A., 1959, An example of non-linear computational instability. *The Atmosphere and Sea in Motion.* Rockefeller Institute Press in association with Oxford University Press, New York, pp. 501–504.

Richtmyer, R. D., 1963, A survey of difference methods for non-steady fluid dynamics. *NCAR Technical Notes* **63**–2. National Center for Atmospheric Research, Boulder, Colorado, 20 pp.